

ULTRAVIOLET AND OPTICAL SPECTRUM STUDIES OF LAMBDA ANDROMEDAE: EVIDENCE FOR ATMOSPHERIC INHOMOGENEITIES

S. L. BALIUNAS¹ AND A. K. DUPREE¹

Harvard-Smithsonian Center for Astrophysics, Cambridge, Massachusetts

Received 1981 May 18; accepted 1981 August 3

ABSTRACT

To pursue the study of solar phenomena in cool stars, we have investigated chromospheric activity in λ Andromedae (HD 222107). This binary, whose primary star is G7–G8 IV–III, shows strong chromospheric emissions and is related to the RS CVn-type systems. We present the first quantitative measurements of chromospheric and solar-type transition-region emissions as a function of the variable starspot and active-region phenomena in an RS CVn star. The presence of optically darker starspots in λ And coincides with the brightening of both Ca II K emission and the ultraviolet transition-region lines. The ultraviolet and optical spectra show attributes of starspots, active regions, and mass flow. Analogies to solar activity are successful in explaining these observations.

Subject headings: stars: binaries — stars: chromospheres — stars: individual — ultraviolet: spectra

I. INTRODUCTION

The understanding of solar-type phenomena occurring on other cool stars is an important step toward the synthesis of solar and stellar physics. By studying solar phenomena on other stars, we expand the range of physical parameters that can influence chromospheric activity. These include age, chemical composition, rotational velocity, and magnetic field strengths. By observing other stars, we will be able to systematically examine the interplay of these parameters and their relation to chromospheric and coronal activity.

The close, but detached, late-type components of RS Canum Venaticorum binaries show behavior reminiscent of sunspot and solar active and flare regions. Nonthermal centimeter radio bursts along with simultaneous X-ray, Ca II, and H α surges have been documented in the RS CVn-type system HR 1099 (Walter, Charles, and Bowyer 1978*a, b*; Hall 1978, and papers following). Strong, variable optical and ultraviolet chromospheric emissions, enhanced by factors of 10–100 in surface fluxes over those in the quiet Sun, have been observed (Weiler 1978; Baliunas and Dupree 1979; Dupree *et al.* 1979). These disk-averaged surface fluxes are comparable to those observed in solar active and flare regions, and the stellar fluxes may be substantially higher if the dominant emitting regions are restricted to only a fraction of the stellar surface.

A significant optical property of the RS CVn variables is the existence of cyclic fluctuations in broad-band light. In *V* band they show amplitudes between a few and about 30% and periods which can be near the

orbital period for the closer binary systems. These continuum modulations can have somewhat variable amplitudes and periods, and long-term observational programs are currently undertaking the detailed study of the light curves, which is thought to be due to starspots (cf. Eaton and Hall 1979). Presumably, starspots which are darker in broad-band optical wavelengths appear on one region of the cooler star which rotates to produce the light modulation. Long-period drifts of the period and phase of the light curve may signify the motion of spots through latitude zones which rotate differentially. The variable amplitude of the light curves may be interpreted as, for example, changes in the size, number, and projected area of the spots on the stellar surface (Hall 1972, 1976; Eaton and Hall 1979).

The system λ And (orbital period 20.5 days; Gratton 1950) is a member of the “long-period” RS CVn stars which have orbital periods longer than 2 weeks. The primary of λ And is classified as G7–G8 IV–III, and is slightly more luminous than the components in the shorter-period RS CVn systems. The companion of λ And is spectroscopically unseen. The *V*-magnitude variations have a period of ~ 54 days (Calder 1938; Archer 1960; Landis *et al.* 1978), an assumed rotation rate which is not synchronous with the orbital period of 20.5 days, as in the shorter-period RS CVn systems. The *V*-band amplitude is in the range of ~ 20 –30%. Since the broad-band light cycle is so prominent, and deep, geometric eclipses in the light curve are absent in λ And, we examined the light curve spectroscopically in the visible and ultraviolet spectrum regions. We find that the calcium emission as well as the higher temperature transition-region fluxes observed from *IUE* are substantially enhanced during minimum light of the system.

¹Guest Observer, *International Ultraviolet Explorer* satellite.

The appearance of cooler inhomogeneities with enhanced chromospheric emission is interpreted as star-spots and associated stellar active regions, and is consistent with a sunspot and solar active-region analogy. Additionally, we examine short- and long-term profile variations in the Ca II K cores and search for similar fluctuations in Mg II.

II. OBSERVATIONS

Two nights in 1978 December 16 and 1979 January 11 were devoted to short-exposure spectra of the Ca II K line ($\lambda 3934$) in λ And. These spectra were obtained to investigate both the maximum and minimum of the broad-band light curve within one cycle and the detailed nature of flux variations in the H and K emission cores apparent in the spectrophotometry of Baliunas *et al.* (1981). In addition, high-resolution Mg II *h* ($\lambda 2803$) and *k* ($\lambda 2796$) spectra were obtained with the *IUE* satellite simultaneously with the 1978 December ground-based observations. We supplement these spectra with the high-resolution profiles of Ca II K covering the period 1974–1979 (Baliunas and Dupree 1979; Baliunas 1979) and additional Mg II spectra obtained in 1978 July 12 and 1979 October 12. The short-wavelength ultraviolet spectra were obtained with *IUE* in 1978 December 16 and 1979 October 11–12. The data from these three spectrum regions are discussed separately below.

a) Calcium II K

The Ca II K spectra were obtained with the echelle and intensified Reticon detector system on the 1.5 m telescope at Mount Hopkins Observatory on 1978 December 15 and 1979 January 10. The resolution of the spectra is ~ 40 mÅ. The spectra have been corrected for the fixed pattern of the detector with sums of several incandescent lamp exposures obtained during the daytime bracketing the observations. This flat-field correction also divides out the instrumental response and spectrograph blaze functions. Perpendicular to the dispersion direction, the astigmatically widened echelle order spans the height of both lines of the Reticon elements. These two lines are summed to produce one spectrum. Due to the tilt of the cross-dispersion grating, there is a slight rotation of the spectral lines perpendicular to the dispersion. This causes a slight shift in the registration of the spectrum between the two lines of the detector elements. This mismatch is identified from the narrow comparison-line spectra, and is at most 1.7 pixels between the two lines of the Reticon. This small shift is less than the instrumental resolution (~ 2.5 pixels), but was applied to the data before adding the two lines of the spectrum.

To convert the spectra to a wavelength scale, thorium-argon lamp exposures were obtained. A fifth-order polynomial solution determined from the location and

wavelengths of the thorium and argon lines gives the transformation of pixels to wavelengths. We typically fit 25–30 lines along the echelle order encompassing the wavelength region 3915–3950 Å. The residuals from the fifth-order fit are examined to detect any curvature which would contribute to systematic errors in the wavelength solution. The residuals of the fits are flat along the echelle order. Over the course of a night, instrumental flexure through large excursions in hour angle may cause a shift of the registration of the spectrum along the detector. This shift, however, is a zero-point adjustment in the central region of the projected spectrum at moderate hour angles; this shift was at most 5 pixels between any two spectra during one night. We thus chose to minimize the time between stellar exposures and obtain comparison lamp spectra only occasionally. The central spectral range of ~ 5 Å inclusive of the K emission core is analyzed. In this region, the spectra are aligned and normalized as described below. We emphasize that bracketing exposures of the comparison lamp show wavelength solutions which have at most a small, linear offset in wavelength in the K core region throughout these observations. Thus, our measurements will not be distorted by elasticity in the mapping of pixels to wavelengths.

Relative flux measurements in the nearby continuum and in the emission cores are calculated. During the observations, the position of the emission core was centered in wavelength to occur where the blaze is fairly flat. The flat-field reduction procedures, combined with the normalization in the wings surrounding the region of the Ca II K emission, reduces any residual effects of the blaze function or instrumental response in introducing any distortions in the shapes of the profiles.

The relative continuum flux, C , has been measured by the following procedure. First, the spectra are reregistered by aligning the short-wavelength edge of the K core, in the absence of suitable photospheric absorption lines in this region. The same photospheric region of each spectrum is normalized to unity in order to intercompare a region of the photospheric spectrum which should remain constant with time. The normalizing region consists of two passbands located in the wings of the photospheric Ca II K absorption profile exterior to the emission core. The average signal in these two 1 Å wide passbands in the wings is used to normalize the spectra. A third 1 Å wide passband is chosen in the wings of the absorption profile, and the flux in this region is calculated and defined as C . These values are plotted in the form of an instrumental magnitude in Figure 1 for both the 1978 December and 1979 January profiles. The values of C for 1978 December and 1979 January are similar throughout and between the observations.

An error estimate is determined from the standard deviations of the mean of the continuum measurements. We compare the standard deviation of C to that ex-

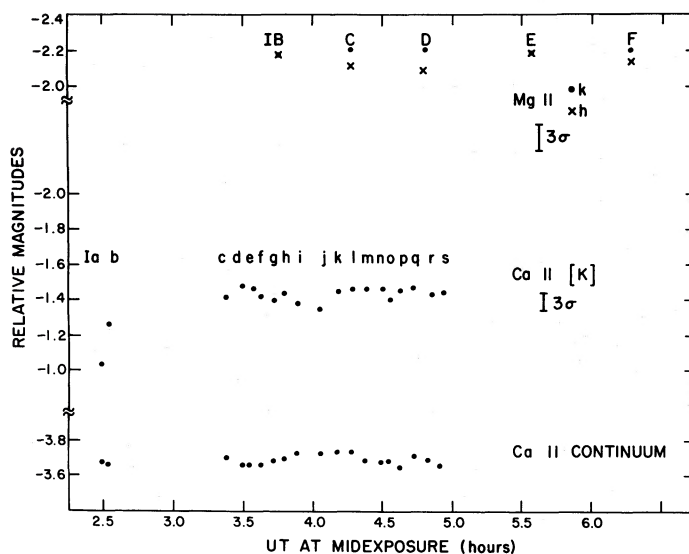


FIG. 1a

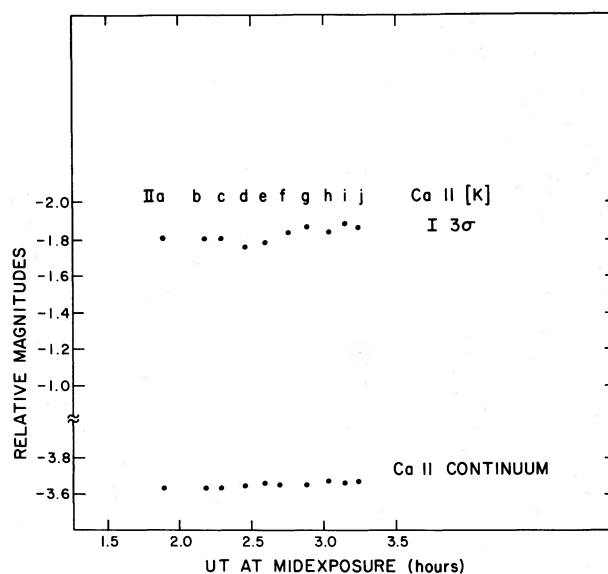


FIG. 1b

FIG. 1.—Relative magnitudes for λ And. The emission index [K] for Ca II is plotted as a function of time for (a) 1978 Dec 16. The fluxes for the Mg II *k* and *h* profiles are also included in relative magnitudes. Note the near constancy of Mg II and simultaneous Ca II K. A 0.4 mag increase in flux was observed between 2.5 and 3.5 hr, prior to the Mg II observations. In (b), [K] is shown as a function of time on 1979 Jan 11. A brightening of [K] occurred over the 1.5 hr span of the data. The sequence numbers of the profiles are included for comparison to Fig. 2.

pected from Poisson statistics. The photon-counting error in the passband of C is evaluated. This error includes the propagated error due to the uncertainty introduced by the normalization. The photon-statistical error is nearly identical compared to that determined from the standard deviation of the mean of C. Additionally, the equivalent width of a photospheric absorption feature near the normalization region has also been

calculated. The equivalent widths also show scatter as expected for photon statistics. We therefore assume that the uncertainty along the spectrum will be given by photon statistics. For the low count rates with which these spectra were obtained, the detector performs extremely well as a photon-counting device.

To define the emission index [K], the spectra are renormalized to unity at the base of the emission core in

two 1 Å wide regions surrounding the emission, and the flux above this continuum is integrated under the profile. These values, converted to an equivalent width in units of angstroms for comparison with the published data of Baliunas and Dupree (1979), are shown in magnitudes in Figure 1. The 3σ error bars for these quantities, as determined from the standard deviations of C , are also shown. As demonstrated by the error analysis, the significant changes in the profiles between the 1978 and 1979 observations are not due to uncertainties in the normalization. Instrumental effects may also be ruled out as causes for the variability. The comparison lamp spectra exposed through the observing intervals do not degrade in resolution or focus with time. Further, equivalent widths of photospheric lines normalized to the wings of the calcium line repeat within the photon statistics.

b) Magnesium II k and h

Five Mg II h and k profiles were obtained during the interval of Ca II observing in 1978 December; other Mg II data were obtained during 1978 and 1979. The Mg II profiles were obtained with the LWR camera aboard the *IUE* satellite (Boggess *et al.* 1978) at high resolution (~ 0.2 Å) and with 5 minute integrations in the large aperture. Corrections for both the background flux and the blaze of the spectrograph have been made. In converting to absolute fluxes, we have multiplied the measured high-resolution fluxes by 100. This calibration factor was determined from nearly simultaneous low-

and high-resolution spectra of λ And in Mg II obtained with the large aperture on 1978 July 12 (Baliunas 1979), and is consistent to within 5% of that of other calibrations (Cassatella *et al.* 1980; Hartmann, Dupree, and Raymond 1981). The integrated fluxes of the h and k lines from 1978 December are included in relative magnitudes along with the Ca II [K] measurements in Figure 1. The Mg II fluxes do not vary by more than 5%, approximately the expected repeatability of the high-resolution *IUE* spectral data (Boggess *et al.* 1978). During this night, no variability in the Mg II fluxes was observed. This behavior is consistent with that of the Ca II profiles: the Ca II measurements nearest in time to the Mg II observations are also all constant to within 5% of the measurements of [K].

c) $\lambda\lambda 1200-1950$ Spectra

Low-dispersion, short-wavelength *IUE* spectra were obtained at extrema in the photometric light curve in 1978 December (light maximum) and 1979 October (light minimum). Strong emissions, typical of those observed in both quiet and active Sun ultraviolet spectra, are apparent. Most of these lines are formed in a temperature range between 20,000 and 100,000 K and are characteristic of solar transition-region lines. The surface fluxes for both phases of the light curve observed from the primary star in λ And are calculated from the angular diameter $\theta = 0''.002539$ (Baliunas 1979) and are listed in Table 1. Two spectra were obtained in 1979 October and fluxes of unsaturated features have been

TABLE 1
PHASE DEPENDENCE OF SHORT-WAVELENGTH ULTRAVIOLET EMISSION
FROM λ AND COMPARED TO THE SUN

LINE	λ	$F_{\oplus} (\times 10^{-13} \text{ ergs cm}^{-2} \text{ s}^{-1})^a$		ENHANCEMENTS ^b		
		0P48 Spot Min	0P02-0P04 Spot Max	Spot Max Spot Min	Spot Min Quiet Sun	Spot Max Quiet Sun
C III	1175	9.5	16	...
N V	1240	4.1	5.9	1.4	13	18
O I	1304	34	51	1.5	22	34
C II	1335	11	16	1.4	6.2	9.1
O I	1357	3.0	4.0	1.3	23	32
Si IV	1394, 1403	8.8	17	1.9	12	22
C IV	1549	21	31	1.5	10	14
He II	1640	13	18	1.4	27	37
C I	1657	9.3	13	1.4	4.6	6.3
O III + Al II	1666, 1670	3.2	3.1	1.0	5.6	5.5
Si II	1808	8.4	11	1.3	3.6	4.8
Si II	1817	...	17	4.6
Si III	1892	4.1	6.0	1.5

^aFlux observed at Earth. The fractional phases were calculated from the ephemeris $\text{JD } 2,443,886.0 + 54^d 2$. Light minimum occurs at phase 0.0. The exposure at spot minimum was SWP 3613. Two spectra (SWP 6828 and 6842) separated by 1 day were obtained at spot maximum. Either the average of two flux measurements or the flux from an unsaturated feature is listed. A dash indicates no measurement. Although the peaks of the Si IV doublet are resolved, the features are not easily separable and the fluxes have been combined.

^bThe surface flux at the primary star has been calculated from the angular diameter of $0''.002539$ (Baliunas 1979). The fluxes for the quiet Sun are tabulated by Linsky *et al.* 1978.

averaged. We calculate the homogeneous surface fluxes although there are obvious surface inhomogeneities modulating the continuum light. It is difficult to disentangle the relative contributions from the emitting regions without knowledge, for example, of the fraction of the surface covered by such emitting regions and the contrast of the "active" regions relative to the "quiet" regions. Nonetheless, it is noteworthy that the homogeneous surface fluxes are comparable to those in the active Sun (Dupree *et al.* 1973) and that the ultraviolet emissions, integrated over the entire disk, are enhanced at light minimum relative to light maximum. The behavior of the emissions with photometric phase is discussed below.

III. RESULTS

a) Short Time Scale Behavior of Calcium II and Magnesium II

Within the 1978 December Ca II K data, there is a large initial increase in the emission (0.4 mag) during the first hour, prior to the Mg II data obtained that night. Significant variations (0.1 mag) occur over the following 2 hours. In the 1979 January data short-term fluctuations, up to 0.1 mag, occurred in less than half an hour. During these intervals, the values of C remain constant within the expected statistics. These smaller variations are similar in time scale and amplitude to those seen spectrophotometrically by Baliunas *et al.* (1981).

For these relative flux changes, we next investigate the detailed changes in the profiles. In Figure 2, selected smoothed, normalized, and subtracted pairs of profiles are presented. For these time derivatives, 2σ error bars are indicated for both the continuum and core regions. These error bars are the quadratic sum of the errors from both spectra determined by photon statistics which include the effects of smoothing the profiles. The length of these error bars encompasses nearly all the excursions from zero in the continuum regions.

The time-derivative profiles show that flux changes can be accompanied by complex profile changes. The profile changes are interpreted as occurring in the stellar atmosphere rather than the interstellar medium. Baliunas and Dupree (1979) had reported that, as expected from the cosmic abundance of calcium and the proximity of the star to the Earth, no interstellar absorption could be detected in the Ca II profiles of λ And. In the 1978 December data, (Ia–Ib) shows that both red and blue emission peaks increased but the depth of the central reversal remained constant. The profile Ib also shows an increased width, but due to the alignment procedure we cannot extract velocity information concerning the edges of the profile. In (Ib–Ic), the blue peak increased faster than the red, and the depth of the central absorption increased in flux. Thereafter, the

profiles remained similar in shape, but overall flux changes occurred. One set of Mg II h and k profiles (Ic) are shown with the two bracketing Ca II K profiles (Ik–Il). The Mg II h and k profiles appear with the same asymmetry noted for Ca II: the red peak is slightly brighter than the blue. Although this asymmetry is weak, it is present in all the individual 1979 December profiles. The asymmetries of both the Mg II and Ca II profiles are statistically significant. As mentioned previously, the reduction and normalization of the Ca II K profiles and their proximity to the midrange of the order reduces the possibility that the blaze function has distorted the profiles. In the case of the Mg II profiles, the blaze correction has been applied.

Some time-derivative profiles for the 1979 January Ca II spectra are shown in Figure 2. The data show a gradual increase in emission beginning at 2.5 hours. As evidenced by (Ile–IIh), the blue peak increased faster than the red, but the sense of the asymmetry is preserved.

Several differences appear between the Ca II 1978 December and 1979 January data. First, the 1979 January data all show a larger flux relative to the base of the K core, although values of C remain similar. Second, the 1978 December Ca II profiles predominantly show the blue peak suppressed relative to the red, or occasionally show peaks of equal strength. In contrast, the 1979 January Ca II data all show the red peak suppressed relative to the blue. The absorption reversal in Ca II K sometimes appears red- or blueshifted from the center of the emission by up to $\sim 10 \text{ km s}^{-1}$. The shape of the 1979 January Ca II profiles is similar to the majority of those reported by Baliunas and Dupree (1979).

b) Correlation of Calcium II with the Optical Light Curve

The two sets of spectra described above, from 1978 December and 1979 January, were obtained at maximum and minimum light, respectively (Fig. 3). The photometric observations were made with an interference filter with an intermediate-width passband centered on the stellar continuum near $\lambda 6575$ (Guinan 1979). From the values of [K] in Figure 1, and from the superposition of two spectra shown in Figure 4, it can be seen that the relative fluxes of the Ca II K emission are brightest at light minimum by a range of 40% to a factor of 2.

In order to further examine this anticorrelation of emission strength with broad-band light, we have incorporated other measurements of [K] from Baliunas and Dupree (1979) and Baliunas (1979). The data plotted as a function of fractional photometric phase ϕ are shown in Figure 5. The phase ϕ was calculated from the ephemeris JD 2,443,886.0 + 54.2 (Hall 1979), where $\phi = 0.0$ corresponds to light minimum. Although the ampli-

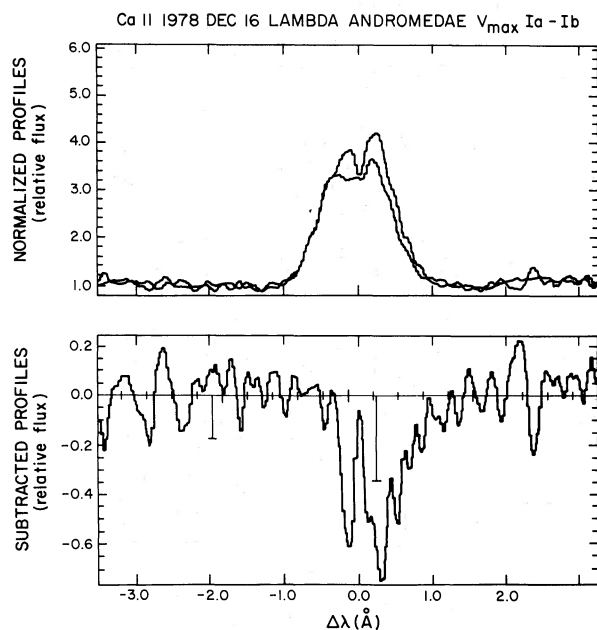


FIG. 2a

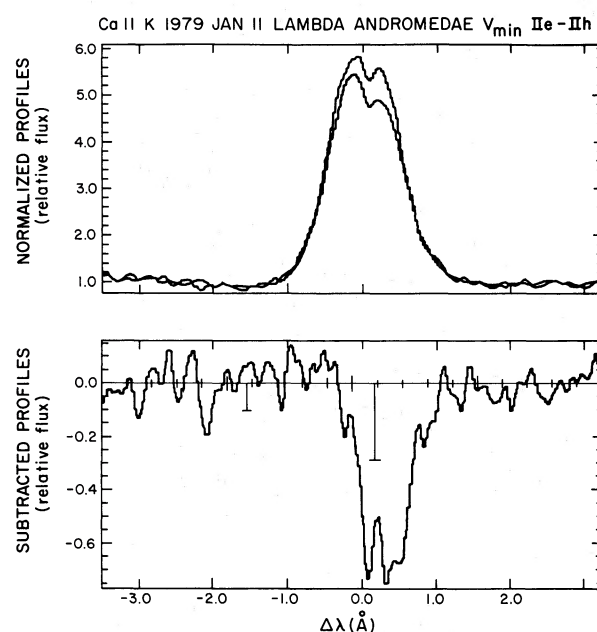


FIG. 2c

FIG. 2.—(a, b, c) Selected Ca II K profiles from Fig. 1 for 1978 Dec 16 and 1979 Jan 11 are shown as pairs of smoothed, normalized profiles along with the difference (in the chronological sequence listed) of the pairs as a function of wavelength. The times and sequence numbers for these profiles are given in Fig. 1. The 2σ error bars for the time derivatives are shown. One set of Mg II *h* and *k* profiles along with the pair of bracketing Ca II exposures is plotted to show the similarity in the asymmetries of the emission peaks for Dec 16. All of the K cores observed during 1979 Jan 11 showed the violet peak brighter than the red.

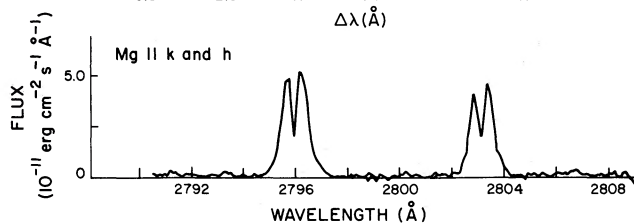
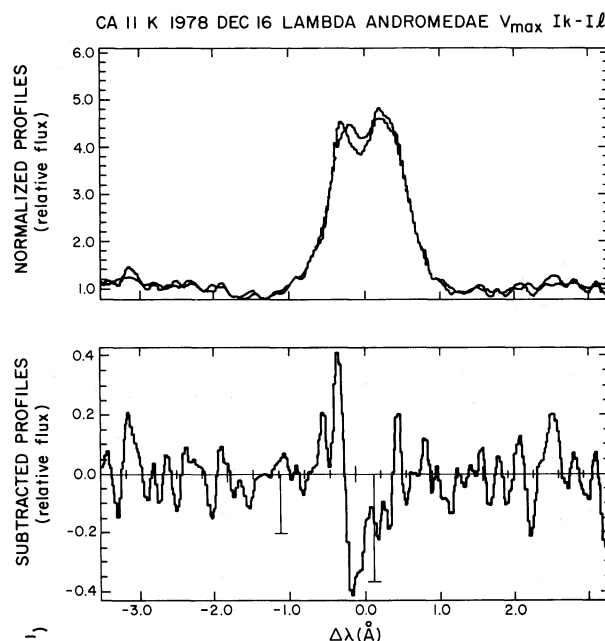


FIG. 2b

tude and shape of the broad-band light curve vary, the minima have remained at nearly constant phase during 1976–1979 (Hall 1979; Guinan 1979). If the ephemeris is extrapolated back to the photometric data of Calder (1938), the minima drift substantially in phase. In the following, we assume that the phases remained constant from 1974–1976 as well. In Figure 5 we discriminate the values of [K] according to decreasing accuracy of ϕ in the following way: (1) those measurements made during a fairly complete light cycle; (2) values of ϕ interpolated between light cycles; (3) for some of the earlier 1974 measurements of Baliunas and Dupree (1979), the ephemeris has been extrapolated.

Figure 5 shows that at light minimum the relative flux in the emission core is larger by $\sim 25\%$ to a factor of 2 than at light maximum. Our measurement of [K] should be a close estimate of the radiative losses in this chromospheric region for relatively cool stars with large emission cores such as λ And. In this case, the additional contribution to the radiative losses underneath the K core should be negligible.

The periodic variation in the continuum light may appear to be a source of systematic modulation in [K] as a function of light-curve phase. In these disk-integrated

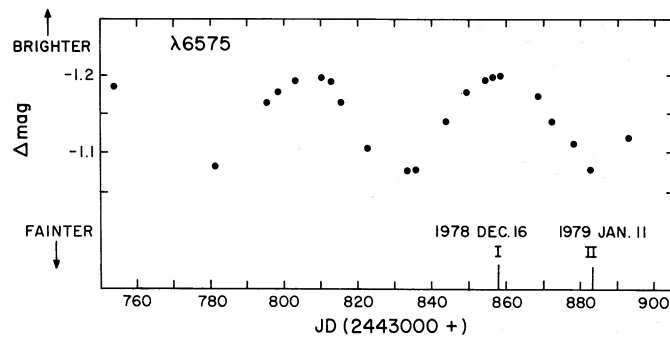


FIG. 3.—Photometric light curve of λ And, showing 1978-1979 data concurrent with the 1978 Dec and 1979 Jan spectra. Differential measurements against ψ Per are given; continuum light brightens upward (Guinan 1979).

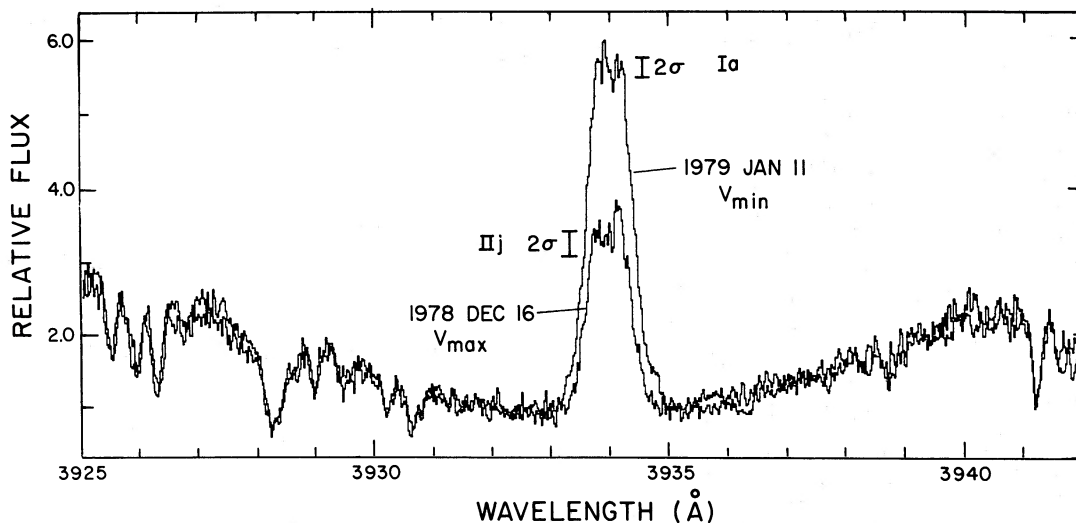


FIG. 4.—The λ And Ca II K unsmoothed, normalized profiles Ia (1978 Dec 16) and IIj (1979 Jan 11) superposed to show the difference in the K core from spot minimum (fainter core) to spot maximum. The 2σ error bars per resolution element for Poisson statistics in the unsmoothed spectra at the level of the line core are shown. The profiles have been shifted in radial velocity for the superposition.

spectra, however, the continuum modulation at the base of the emission core will be weak. In the spatially unresolved observation of the visible disk, light from the brighter portions of the photosphere will easily contaminate and dominate the surface flux from the faint, photospheric regions of the spots. Thus, the normalization of the Ca II K emission to the nearby photospheric region will not systematically skew [K] as a function of light-curve phase.

We have also searched for correlations of [K] with the 20.5 day orbital period. The radial-velocity curve was checked with the photospheric lines in the K and H regions of the spectra of Baliunas and Dupree (1979) and Baliunas (1979). The line positions agree well with the phase and radial velocity derived from the elements of Walker (1944) and Gratton (1950). Comparing [K] as a function of orbital phase, we find no systematic trend. This is clearly exhibited by the points between fractional

spectroscopic phases 0.0 and 0.20. Most of the range of [K] is observed in this small range in orbital phase. This result is not surprising, as discussed by Baliunas and Dupree (1979). Since λ And has a small mass function, the system is probably oriented close to, but not exactly, pole-on to the line of sight. In this orientation, where the probability of geometric eclipses is small, the cause for variations is likely due to the contrast of an inhomogeneous surface rotating through our field of view.

In Figure 5 we have also shown visual estimates in the collected spectra of V/R , the ratio of the violet to red emission peak as a function of light curve phase. We differentiate between $V < R$, $V = R$, and $V > R$, and an intermediate appearance where the central absorption reversal is not sharply defined but the profile is significantly asymmetric. A weak correlation is seen: $V < R$ occurs only at light maximum; $V > R$ is seen at light minimum, but can occur at other phases except spot

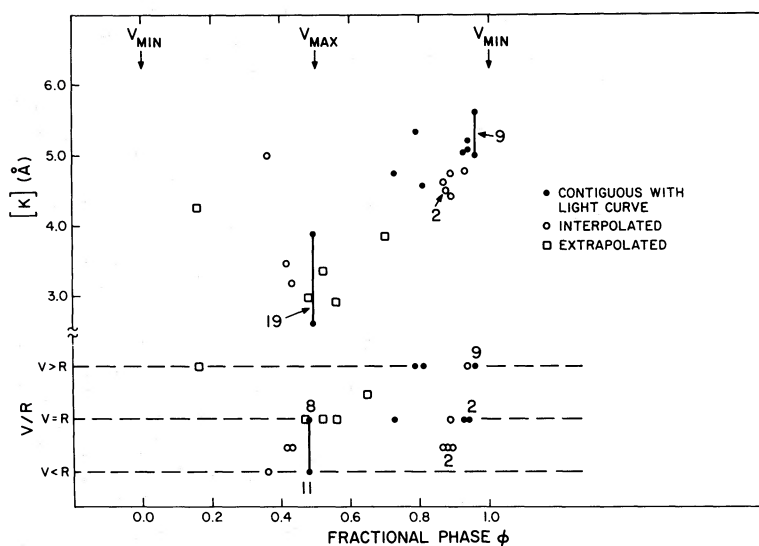


FIG. 5.—Ca II [K] in λ And as a function of the 54 day light-curve phase ϕ . Extrema of the light curve are noted. The symbols indicate whether or not concurrent photometry is available for the spectra. A bar indicates the range of activity observed during a night, a number near a symbol indicates the number and spectra which contribute to the measurement. The lower graph shows the ratio of the violet-to-red emission peaks as a function of ϕ .

minimum. The appearance of the asymmetries in both Ca II and Mg II will be discussed below.

The behavior of [K] as a function of photometric phase in Figure 5 is significant for the following reason: the solid bars indicate the range of numerous spectra obtained on two nights corresponding to maximum and minimum during one cycle that was well observed photometrically. These data clearly show the increase in relative Ca II K flux at light minimum. For all the spectroscopic observations shown in Figure 5, the fact that this correlation persists may indicate that the lifetime of the star-spot region is 3 years, and possibly 5 years if the extrapolation of phases to 1974 is reliable. Further, the short time scales of the variations observed on individual nights and the time scales observed by Baliunas *et al.* (1981) indicate that a limited region of the disk dominates the emission. Variability in the range of the emission may appear at any phase. This may be indicative of flarelike activity over the many cycles observed.

c) Magnesium II versus Photometric Phase

The phase coverage for Mg II is more sparse. Table 2 lists the fluxes in Mg II *k* and *h* obtained here with *IUE* compared with those of Baliunas and Dupree (1979), which were observed with the *Copernicus* satellite. If the accuracy of the data between the *Copernicus* and *IUE* systems is assumed to be $\sim 20\%$, we see no variability in the fluxes even at minimum light compared to maximum. The fluxes have been calculated by summing the signal between the base of the emission core. Little, if

any, photospheric emission will affect the assessment of either the chromospheric radiative losses or their variation. We have also included in Table 2 the data of Basri and Linsky (1979) which may suggest a fading of emission near maximum light. The Basri and Linsky data have been reduced by a factor of 1.35 to account for the difference between our derived calibration factors for the *IUE* LWR camera.

The behavior of the Mg II *h* and *k* *V/R* asymmetries as a function of light phase is consistent with that of Ca II K (Fig. 6). However, the chromospheric asymmetries of the Mg II emission cores are difficult to measure. The line profile arising from the binary system may be affected by interstellar absorption in such a way as to mimic intrinsic asymmetry changes. The velocity difference of the primary star between the two orbital phases amounts to $\sim 8 \text{ km s}^{-1}$ —too small to measure easily with *IUE*. However, the sense of the stellar motion (1978 Dec 16 corresponds to $V_R \sim +11 \text{ km s}^{-1}$ and 1979 Oct 12 corresponds to $V_R \sim +3 \text{ km s}^{-1}$) is consistent with interstellar modulation of the asymmetry.

We can assume that the central absorption feature arises from the interstellar emission. By taking a local continuum defined by the emission peaks, we measure equivalent widths of 133 mÅ and 117 mÅ for the $\lambda 2795$ and $\lambda 2802$ lines, respectively. These values are larger than our earlier measures from *Copernicus* spectra at lower dispersion (Baliunas and Dupree 1979). If attributed to interstellar absorption, they are consistent with the range of values cited by Kondo *et al.* (1978) and Bohm-Vitense (1981) for stars 25 pc distant. The column density of Mg II implied by the equivalent

TABLE 2
MAGNESIUM II FLUXES IN LAMBDA ANDROMEDAE

Copernicus Observations ^a						
UT Date	JD	ϕ	Surface Flux at Earth (ergs cm ⁻² s ⁻¹) ($h+k$)	Surface Flux from Primary (ergs cm ⁻² s ⁻¹) ^b ($h+k$)	V/R^c	
1974 Dec 21/22	2,442,404	0.65	1.6(-10)	4.2(6)	...	
1976 Oct 9/10	2,443,062	0.79	1.6(-10)	4.2(6)	...	
IUE Observations						
UT Date	LWR	JD	ϕ	Surface Flux at Earth (ergs cm ⁻² s ⁻¹) ^d ($h+k$)	Surface Flux from Primary (ergs cm ⁻² s ⁻¹) ^b ($h+k$)	V/R
1978 Jul 12	1823	2,443,702.1	0.61	1.5(-10)	4.0(6)	$V > R$
1978 Aug 26 ^e	2178-9	2,443,746.9	0.43	1.3(-10)	3.3(6)	...
1978 Dec 14	3162	2,443,856.7	0.48	1.4(-10)	3.7(6)	$V < R$
1978 Dec 16	3179-82	2,443,858.7	0.52	1.4-1.5(-10)	3.7-4.0(6)	$V < R$
1979 Oct 12	5817	2,444,158.9	0.04	1.5(-10)	4.0(6)	$V > R$

^aBaliunas and Dupree 1979.

^bAngular diameter 0'002539 (Baliunas 1979) used to calculate the stellar surface flux from the primary star.

^cResolution of *Copernicus* profiles was insufficient to resolve peaks.

^dCalibrated to low-dispersion fluxes at Mg II (see text).

^eObservations from Basri and Linsky 1979. The fluxes have been recalculated with the calibration factor for the high resolution LWR data determined here.

widths of $\lambda 2795$ is 9.4×10^{12} cm⁻², assuming $b = 5$ km s⁻¹. The line lies on the flat part of the curve of growth and a large uncertainty results in the column density. If, for instance, $b = 7.5$ km s⁻¹, then $N_{\text{Mg II}} = 5.1 \times 10^{12}$ cm⁻².

It is not obvious whether this feature results completely from interstellar absorption or not. The solar Mg II profile at disk center (Kohl and Parkinson 1976) exhibits a more narrow reversal (0.20 Å vs. 0.25 Å at half-power absorption) and peak separation (0.320 Å vs. 0.570 Å) than λ And. Larger values of these quantities can be expected from subgiants like λ And than from dwarf stars. Other observations of Mg II suffer from a lack of corresponding Ca II measures. For instance, an exposure of λ And near maximum of light phase (0.43) yet near orbital phase 0.76 (Basri and Linsky 1979) would be expected to show a profile similar to the 1978 December 16 ($V < R$) profile, if the asymmetry were intrinsic to the star; however the asymmetry is reversed ($V > R$), consistent with interstellar modulation. The Ca II asymmetry at the time was not measured. Further sampling of the profile is desirable to identify the dominant effect.

The behavior of Mg II flux as a function of light curve phase is difficult to assess because the sampling of data is limited. At first glance, it appears that the total flux of the Mg II feature is constant to within 7% between light curve minimum (1979 Oct 12) and maximum (1978 Dec 14-16). In contrast, Ca II K can vary as much as a

factor of 2 between light curve extrema. However, except for 1978 December 14-16, there are no simultaneous measurements of Ca II and Mg II as a function of phase. In addition, due to the lack of sampling statistics for Mg II and the possibility that unpredictable short-term changes may occur, the discussion of the behavior of Ca II and Mg II must be deferred until a larger data base is obtained.

d) Transition-Region Spectrum versus Photometric Light Curve

The surface fluxes of the ultraviolet emissions accessible to the short-wavelength region of *IUE* are generally enhanced by 30-50% at light minimum compared to light maximum (Fig. 7). The surface fluxes for the transition-region lines are not affected by the photospheric light modulation. On the Sun, the enhancement of ultraviolet emissions in sunspots and associated active regions is pronounced (Dupree *et al.* 1973; Foukal *et al.* 1974; Foukal 1976; Cheng, Doschek, and Feldman 1976). The ratios of the fluxes at maximum and minimum phases are also listed in Table 1. At spot minimum, the homogeneous surface fluxes are brighter by factors of 4-30 than the quiet Sun, while at spot maximum, surface fluxes brighten by factors of 5-40.

The ultraviolet spectra of λ And show attributes of both starspots and active regions. In the Sun, emis-

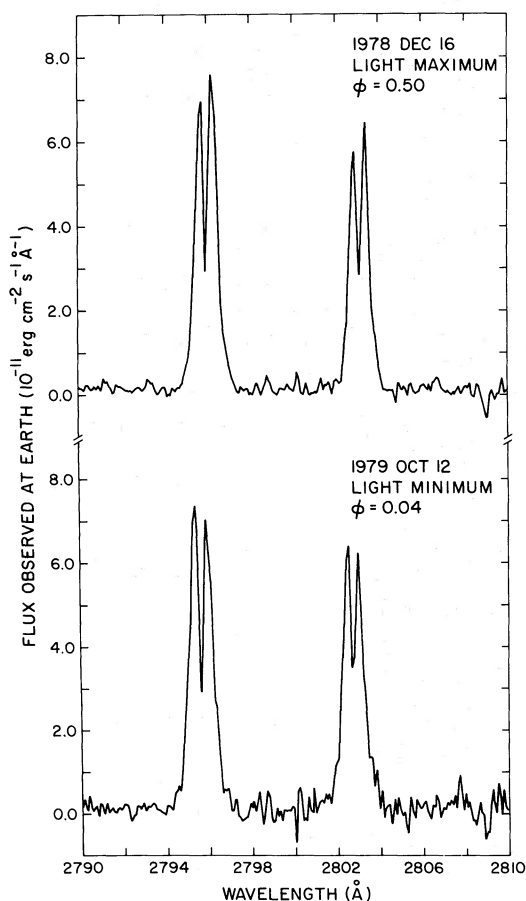


FIG. 6.—Changes in the asymmetry of the Mg II *h* and *k* profiles for partially spotted ($V > R$) and unspotted ($V < R$) regions in λ And. The profile from 1978 Dec 16 is the smoothed average of all five obtained that night.

sion from ions formed in the temperature range $10^5 < T(K) < 10^6$ are brighter over sunspot umbrae than in surrounding plages (Foukal *et al.* 1974). Most of these sunspot signatures (O IV $\lambda 554$, O VI $\lambda 1032$, Ne VII $\lambda 465$, Mg VIII $\lambda 430$) are inaccessible to *IUE*. In this temperature range, the presence of starspots is suggested by N V ($\lambda 1240$, $T = 2 \times 10^5$ K) and C IV ($\lambda 1550$, $T = 1 \times 10^5$ K), which brighten in λ And at spot maximum. However, He II ($\lambda 1640$) is weak over sunspot umbrae (Cheng, Doschek, and Feldman 1976), while in λ And the strength of He II increases at spot maximum. This feature appears strongly over active regions, presumably owing to its formation following photoionizations by the bright EUV continuum over active regions (Hartmann *et al.* 1979). Upper limits of nondetection for the O VI ($\lambda 1032$) feature were obtained nearly at spot maximum and minimum from the *Copernicus* satellite (Baliunas and Dupree 1979). We estimate the expected O VI ($\lambda 1032$) emission at spot maximum by scaling sunspot and solar active-region measurements of O VI relative to C II ($\lambda 1335$) (Dupree *et al.* 1973; Foukal *et al.* 1974).

The predicted O VI flux is about 15 times smaller than the upper limits observed.

We estimate the pressure in the transition region over the spotted and unspotted hemispheres from the surface fluxes of the collisionally dominated, optically thin emissions. For active chromosphere stars such as λ And, we expect thermal conduction to dominate in the transition region which leads to a scaling law for the transition-region pressure of a star relative to the Sun (Haisch and Linsky 1976). Several line ratios have been omitted from the determination of the pressure for the following reasons. In the high temperature species, for example, in C IV and N V, the enhancement is increased due to the role of conduction in dominating the radiative losses. This has been described for solar active regions as compared to the quiet Sun (Dupree *et al.* 1973) and other active chromosphere stars observed with *IUE* (Dupree *et al.* 1979). Additionally, N V is usually blended with the wings of Ly α in the low dispersion mode of *IUE*. The O I lines ($\lambda 1304$) may be controlled through radiative excitation by Ly β (Haisch *et al.* 1977). The He II ($\lambda 1640$) emission may be enhanced by recombinations subsequent to photoionization of He II by extreme ultraviolet photons (Zirin 1975; Avrett, Vernazza, and Linsky 1976; Hartmann *et al.* 1979). Finally, the Si II, III, and IV lines are affected through charge-transfer ionization and recombination reactions with H⁺ and He⁺ (Baliunas and Butler 1980). Therefore, for the lower transition-region pressure, we use ratios of C II ($\lambda 1335$), C I ($\lambda 1657$), and metallicity of λ And (Baliunas 1979) to obtain the pressures in the lower transition region to be ~ 1.3 dyn cm⁻² for the unspotted hemisphere and ~ 1.9 for the spotted hemisphere.

e) Profile Asymmetries versus Light Curve Phase

There is a difference in the asymmetry of the disk-integrated profiles of both Mg II and Ca II between the spotted and unspotted regions: the appearance of spots at light minimum shows a profile which has its red peak depressed relative to the blue, while maximum light shows a weaker blue peak than red peak. As discussed above, an intriguing question is the cause of the apparent asymmetry in the Mg II line profiles. The same asymmetry is found in the Ca II profiles measured simultaneously. Although the interstellar absorption in Mg II renders the stellar asymmetry difficult to assess, we would expect that the intrinsic asymmetry of Ca II K is also present for Mg II *h* and *k*. Our coverage of the spectroscopic orbit of λ And in Ca II K is sufficient to determine that the asymmetries are intrinsic to the star. In the following, the evidence for asymmetries relies on the Ca II K measurements, the discussion may be applicable to Mg II in λ And as well.

For the typical sunspot umbral profile, self-reversals are apparent in the majority of high-resolution spectrograms, and the predominant asymmetry is that of $V > R$

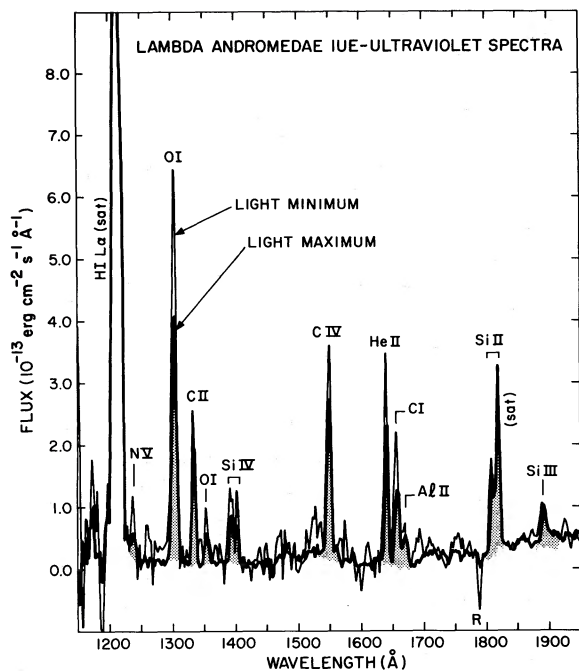


FIG. 7.—IUE spectra of λ And in the short-wavelength region as a function of light curve phase. At light minimum, or the maximum appearance of spots and active regions, the high temperature emissions are enhanced compared to light maximum.

(Engvold 1967; Mattig and Kneer 1978). Quieter umbral regions may show no absorption reversal, but the profiles tend to show another asymmetry: a broad wing on the red edge of the profile. The Ca II profiles in umbral regions strongly exhibit the asymmetry $V > R$. In sunspot flares, much more intense emission is observed. The emission cores are flat-topped and symmetric, but the surrounding penumbral emissions may be asymmetric $V > R$ (Machado and Seibold 1973). Thus, the regions on the Sun associated with sunspots show the same profile asymmetry as seen in λ And at light minimum, strengthening the analogy of solar-like behavior on λ And. The line profiles from λ And represent an integration over various contributions on the visible disk and are difficult to compare directly to the spatially resolved solar profiles. The behavior of the active hemisphere on λ And, nevertheless, is consistent with the behavior over an average of sunspots and solar active regions.

In line-profile calculations for Ca II and Mg II, differential velocity fields in the line-forming regions can produce asymmetric profiles, for example, in an atmosphere which is differentially expanding, the opacity at line center shifts to shorter wavelengths. The red peak emission may appear enhanced as photons escape preferentially in the red wing (Hummer and Rybicki 1968; Gouttebroze 1977). Conversely, the profiles observed with a stronger violet than red peak are suggestive of differential downflows (Durrant, Grossman-Doerth, and

Kneer 1976; Gouttebroze 1977). There is some evidence that the solar atmosphere above sunspots shows velocity inflow. Extreme ultraviolet emissions in the coronae above sunspot umbrae are quite strong in the region $10^5 < T(K) < 10^6$ K. Such enhanced emission persists over relatively long time scales, which implies a steady-state condition. By considering the energy and pressure balance in these regions, Foukal (1976) suggests that the plasma above sunspot umbrae may flow downward along magnetic field lines. Some empirical evidence (Bruner *et al.* 1976) indicates downflows of 30–100 km s⁻¹ observed in extreme ultraviolet C IV ($\lambda 1548$) emissions in the cool regions above sunspot umbrae. This downward motion may be expected to occur as low in the atmosphere as the chromospheric emissions of Mg II and Ca II, and a circulation pattern is evident in the Evershed effect. The relative strength of the asymmetries ($V > R$) shown by the Ca II H and K cores in sunspots can be matched if we infer differential downflows of ~ 10 km s⁻¹ from the calculations of Durrant, Grossman-Doerth, and Kneer (1976). For differential downflows of this magnitude, similar asymmetries in the Mg II line profiles are also predicted (Gouttebroze 1977). Calculated profiles including downflow velocities are in qualitative agreement with the appearance of the Ca II emission cores observed above umbrae (Mattig and Kneer 1978). However, the comparison of the line centers of Ca II and Mg II in disk-averaged stellar profiles with those in solar regions is difficult. The line cores may be affected by a combination of the following:

1. Differences in velocity fields between various solar regions and λ And may exist. For example, substantially larger macroturbulence (projected rotational broadening is expected to be small) in λ And would smear the contrast between the peaks and the central core.
2. The disk-averaging process may have smeared the profiles over inhomogeneities in the stellar case.
3. Increased upper-chromospheric pressures may fill in the line cores and confuse the appearance of the line shapes (Baliunas *et al.* 1979).
4. In the quiet Sun, asymmetries in the Ca II line cores may be due to wave phenomena in the solar atmosphere. For example, line profile calculations indicate that asymmetries may result as the propagation of waves causes perturbations in the density and temperature structure (Cram 1976), or in the deposition of nonradiative heating (Cram, Brown, and Beckers 1977) in the solar chromosphere.

An additional test for downflows over the spot-dominated hemispheres of λ And or other RS CVn stars would be an investigation of the optically thin transition-region lines which may reveal Doppler shifts as a function of height of formation, especially if a restricted region dominates the disk-integrated emission (Baliunas *et al.* 1981).

During maximum light in λ And, outflow of material may be suggested by the K core asymmetries which

show $V < R$. Little direct evidence exists for mass loss in λ And and other RS CVn stars. There are regions of the H-R diagram which show the presence or absence of particular mass-loss indicators:

1. Violet-to-red emission-peak ratios of Ca II which show $V < R$ (Stencel 1978).
2. Circumstellar absorption lines, especially at H and K, blueshifted substantially from line center (Reimers 1977).
3. In the coolest, most luminous stars (e.g., α Ori) there is a lack of high temperature transition-region emissions (C IV, N V) and appearance of strong lines of O I measured with *IUE* (Linsky and Haisch 1979; Dupree 1980).

Although the RS CVn stars do not strongly show these mass-loss indicators, mass loss or mass transfer is probably occurring through flare activity or a stellar wind. The evolutionary status of many RS CVn binaries argues that mass loss or transfer may have taken place from the cooler component; the amount of mass in value may be up to $0.2 M_{\odot}$ for Z Her (Popper and Ulrich 1977). As in λ And, these stars also often show the asymmetry associated with outflow in chromospheric lines. For example, extremely active chromospheric and flare phenomena appear in HR 1099, in which multiple components of Mg II emission can appear at velocities of $< -250 \text{ km s}^{-1}$ from line center (Weiler 1978) or the moderate velocity emission component of Ca II H and K in λ And (Baliunas and Dupree 1979). However, large mass-loss rates ($> 10^{-8} M_{\odot} \text{ yr}^{-1}$), which have been claimed on the basis of orbital period changes (Hall 1972, 1976), would tend to drive the RS CVn stars out of synchronism. Further, the observed soft X-ray fluxes should be self-absorbed by the circumstellar material (DeCampi and Baliunas 1979). Moderate mass loss ($\sim 10^{-9}$ – $10^{-11} M_{\odot} \text{ yr}^{-1}$) is compatible with the X-ray emission measures (Weiler *et al.* 1978). Some luminous K giants, also below the region where high mass-loss rate indicators occur in the H-R diagram, show circumstellar absorption features at high velocities. These stars are suspected to have close companions and/or high rotational velocities (Reimers 1977). Possibly the presence of a companion enhances not only the mass loss but also the strength of chromospheric activity in the RS CVn stars.

IV. DISCUSSION

Although circumstantial, the evidence is overwhelmingly favorable for a picture that is consistent with one of solar analogues. For the RS CVn stars, the analogies of solar features are thoroughly discussed by Eaton and Hall (1979). Vigorous activity, observable in stars with enhanced surface fluxes such as the RS CVn or BY Dra variables, is well suited for studies of solar activity analogues.

As a result of both the inhomogeneous distribution on the Sun of regions bright in K emission and a lifetime of

such regions longer than that of a rotational period, K emission variations of about 15% can be expected due to rotational modulation (Sheeley 1967). The evidence of the photometric wave in integrated light and the near correspondence of the wave period with the expected rotational period implies that intense chromospheric starspot activity may be present in the RS CVn variables. Further, from broad-band color measurements, the redder color at spot maximum indicates spots cooler than the surrounding photosphere. The rotational modulation of broad-band colors, combined with the enhancement of ultraviolet emission lines with surface fluxes similar to those observed over solar sunspot regions, is the strong evidence for starspots and associated active regions in the RS CVn systems.

Some RS CVn systems have been studied spectroscopically to search for a trend of enhanced chromospheric emission with light minimum in the broad-band cycle. The optical indicators observed include Ca II and H α , although the latter is observed in emission in only a few systems. The ultraviolet emissions, Ly α and Mg II, have been studied (Mulligan and Bopp 1975; Bopp and Talcott 1978; Weiler 1978; Weiler *et al.* 1978). Some of these results, however, are suggestive but not conclusive because the search for such trends is hampered by the following systematic effects.

1. Only one or two consecutive cycles of the wave are usually observed. Thus, variability other than that produced by rotational modulation can occur. Especially in the shorter period systems, these fluctuations are more strongly suspect in conspiring to produce a spurious correlation.

2. Often simultaneous broad-band photometry is not obtained along with the spectroscopy. The amplitudes and periods of the waves can be variable (Hall 1976; Chambliss *et al.* 1978).

3. Some of the RS CVn systems undergo geometrical eclipses which substantially confuse the appearance of the photometric wave. Some of the binary systems are double-lined spectroscopic binaries with significant spectral-line contributions from both components. Line blends make assessment of the emission strengths difficult.

We have attempted to reduce these systematic effects in the data presented here. The correlation persists for many cycles over 3 years, and possibly 5 years if the extrapolation of the ephemeris is reliable. Our data provide evidence that Ca II emission is enhanced at light minimum by at least 20% and possibly by a factor of ~ 1.5 , depending on the strengths of the emissions within a given cycle light minimum. Undoubtedly, the colors of the photometric waves indicate that the starspot phenomenon occurs on other RS CVn stars, but much more data over long time scales, such as the spectroscopy of Bopp and Talcott (1978) combined with the photometry of Chambliss *et al.* (1978) in HR 1099, is required to disentangle spot activity from systematic complications

and to quantitatively study the spot phenomenon. Other useful diagnostics include the observation of spectrum features associated with the cooler photospheres of starspots. For example, the observed enhancement of TiO absorptions at light minimum in HR 1099 is evidence that the darker hemisphere is cooler, consistent with the spot model (Ramsey and Nations 1980).

V. SUMMARY

In λ And we observe a correlation of the 54 day photometric wave with Ca II chromospheric emission cores: the flux in the K core is 20% to a factor of 2 larger at wave minimum than at maximum; this effect apparently can persist for 3–5 years. The ultraviolet transition-region emissions are also enhanced at light minimum. These flux enhancements at minimum light are probably due to the influence of starspots. The starspots appear to be cooler than the surrounding photosphere and may cover $\sim 30\%$ of the visible hemisphere. Asymmetries in the line cores may be due to mass motions along the line of sight. Straightforward

interpretation of the line-core asymmetries indicate that mass upflow may take place over the unspotted regions, and, as in sunspots, downflows may occur over the starspots. Short-term flux variations in the K cores observed at spot maximum and minimum can be seen in less than an hour. These changes tend to preserve the prevailing line asymmetry.

At times of spot minimum, the Ca II and perhaps also Mg II lines show asymmetries in the emission peaks which are consistent mass upflows, but which do not necessarily imply escape velocities and thus mass loss. The unspotted regions may be associated with coronal holes from which a stellar wind flows. Higher velocity features, circumstellar features, or Doppler measurements of optically thin ultraviolet emissions would establish the nature of mass flows more firmly.

This work is supported in part by the Langley-Abbot program of the Smithsonian Astrophysical Observatory and NASA grant NAG 5-87. We kindly thank Professor E. F. Guinan for the photometry of λ And prior to publication.

REFERENCES

- Archer, S. 1960, *J. British Astr. Assoc.*, **70**, 95.
 Avrett, E., Vernazza, J. L., and Linsky, J. L. 1976, *Ap. J. (Letters)*, **207**, L199.
 Baliunas, S. L. 1979, Ph.D. thesis, Harvard University.
 Baliunas, S. L., Avrett, E. H., Hartmann, L., and Dupree, A. K. 1979, *Ap. J. (Letters)*, **233**, L129.
 Baliunas, S. L., and Butler, S. 1980, *Ap. J. (Letters)*, **235**, L45.
 Baliunas, S. L., and Dupree, A. K. 1979, *Ap. J.*, **227**, 870.
 Baliunas, S. L., Hartmann, L., Vaughan, A. H., Liller, W., and Dupree, A. K. 1981, *Ap. J.*, **246**, 473.
 Basri, G. S., and Linsky, J. L. 1979, *Ap. J.*, **234**, 1023.
 Boggess, A. *et al.* 1978, *Nature*, **275**, 372.
 Bohm-Vitense, E. 1981, *Ap. J.*, **244**, 504.
 Bopp, B. W., and Talcott, J. C. 1978, *A. J.*, **83**, 1517.
 Bruner, E. C., Jr. *et al.* 1976, *Ap. J. (Letters)*, **210**, L97.
 Calder, W. 1938, *Harvard Obs. Bull.*, No. 405.
 Cassatella, A., Holm, A., Ponz, D., and Schiffer, F. H., III. 1980, *IUE NASA Newsletter*, No. 8.
 Chambliss, C. R., Hall, D. S., Landis, H. J., Louth, H., Olson, E. C., Renner, T. R., and Skillman, D. R. 1978, *A. J.*, **83**, 1514.
 Cheng, C. C., Doschek, G. A., and Feldman, U. 1976, *Ap. J.*, **210**, 836.
 Cram, L. E. 1976, *Astr. Ap.*, **50**, 263.
 Cram, L. E., Brown, D. R., and Beckers, J. N. 1977, *Astr. Ap.*, **57**, 211.
 DeCampi, W., and Baliunas, S. L. 1979, *Ap. J.*, **230**, 815.
 Dupree, A. K. 1980, in *Highlights of Astronomy*, Vol. 5, ed. P. Weymann (Dordrecht: Reidel), p. 263.
 Dupree, A. K., Black, J. H., Davis, R. J., Hartmann, L., and Raymond, J. C. 1979, in *The First Year of IUE*, ed. A. J. Willis (London: University College), p. 217.
 Dupree, A. K., Goldberg, L., Noyes, R. W., Parkinson, W. H., Reeves, E. M., and Withbroe, G. L. 1973, *Ap. J.*, **183**, 321.
 Durrant, C. J., Grossman-Doerth, U., and Kneer, F. J. 1976, *Astr. Ap.*, **51**, 95.
 Eaton, J. C., and Hall, D. S. 1979, *Ap. J.*, **227**, 907.
 Engvold, O. 1967, *Solar Phys.*, **2**, 234.
 Foukal, P. 1976, *Ap. J.*, **210**, 575.
 Foukal, P. V., Huber, M. C. E., Noyes, R. W., Reeves, E. M., Schmah, E. J., Timothy, J. G., Vernazza, J. E., and Withbroe, G. L. 1974, *Ap. J. (Letters)*, **143**, L143.
 Gouttebroze, P. 1977, *Astr. Ap.*, **54**, 203.
 Gratton, L. 1950, *Ap. J.*, **111**, 31.
 Guinan, E. F. 1979, private communication.
 Haisch, B. M., and Linsky, J. L. 1976, *Ap. J. (Letters)*, **205**, L39.
 Haisch, B. M., Linsky, J. L., Weinstein, A., and Shine, R. A. 1977, *Ap. J.*, **214**, 785.
 Hall, D. S. 1972, *Pub. A.S.P.*, **84**, 323.
 ———. 1976, in *IAU Colloquium 29, Multiple Periodic Variable Stars*, ed. W. S. Fitch (Boston: Reidel), p. 287.
 ———. 1978, *A. J.*, **83**, 1469.
 ———. 1979, private communication.
 Hartmann, L., Davis, R., Dupree, A. K., Raymond, J. C., Schmidtke, P. C., and Wing, R. F. 1979, *Ap. J. (Letters)*, **233**, L69.
 Hartmann, L., Dupree, A. K., and Raymond, J. C. 1981, *Ap. J.*, **246**, 193.
 Hummer, D. G., and Rybicki, G. B. 1968, *Ap. J. (Letters)*, **153**, L107.
 Kohl, J., and Parkinson, W. H. 1976, *Ap. J.*, **205**, 599.
 Kondo, Y., Talent, D. L., Barker, E. S., Dufour, R. J., and Modisette, J. L. 1978, *Ap. J. (Letters)*, **220**, L97.
 Landis, H. J., Lovell, L. P., Hall, D. S., Henry, C. E., and Renner, T. R. 1978, *A. J.*, **83**, 176.
 Linsky, J. L. *et al.* 1978, *Nature*, **275**, 389.
 Linsky, J. L., and Haisch, B. M. 1979, *Ap. J. (Letters)*, **229**, L27.
 Machado, M. E., and Seibold, J. R. 1973, *Solar Phys.*, **29**, 75.
 Mattig, W., and Kneer, F. 1978, *Astr. Ap.*, **65**, 11.
 Mulligan, K., and Bopp, B. W. 1975, *Info. Bull. Var. Stars*, No. 1075.
 Popper, D. M., and Ulrich, R. K. 1977, *Ap. J. (Letters)*, **212**, L131.
 Ramsey, L. W., and Nations, H. L. 1980, in *Cool Stars, Stellar Systems, and the Sun*, ed. A. K. Dupree (SAO Special Report No. 389), p. 97.
 Reimers, D. 1977, *Astr. Ap.*, **57**, 395.
 Sheeley, N. R. 1967, *Ap. J.*, **147**, 1106.
 Stencel, R. E. 1978, *Ap. J. (Letters)*, **233**, L37.
 Walker, E. C. 1944, *J.R.A.S. Canada*, **38**, 249.
 Walter, F., Charles, P., and Bowyer, S. 1978a, *Ap. J. (Letters)*, **225**, L119.
 ———. 1978b, *Nature*, **274**, 569.
 Weiler, E. J. 1978, *A. J.*, **83**, 795.
 Weiler, E. J. *et al.* 1978, *Ap. J.*, **225**, 919.
 Zirin, H. 1975, *Ap. J. (Letters)*, **199**, L63.

S. L. BALIUNAS and A. K. DUPREE: Harvard-Smithsonian Center for Astrophysics, 60 Garden Street, Cambridge, MA 02138